The endogenous opioid dynorphin is required for normal bone homeostasis in mice

Paul A. Baldock [a,c,f], Frank Driessler [a], Shu Lin [a], Iris P.L. Wong [a], Yanchuan Shi [a], Ernie Yulyaningsih [a], Lesley Castillo [a], Sonia Janmaat [a], Ronaldo F. Enriquez [a], Ayse Zengin [a], Brigitte L. Kieffer [d], Christoph Schwarzer [e], John A. Eisman [b,c], Amanda Sainsbury [a,g], Herbert Herzog [a,c,f]

[a] Neuroscience Research Program, Garvan Institute of Medical Research, 384 Victoria St., Darlinghurst, Sydney, NSW 2010, Australia[b] Osteoporosis and Bone Biology Research Program, Garvan Institute of Medical Research, 384 Victoria St., Darlinghurst, Sydney, NSW 2010, Australia[c] Faculty of Medicine, University of NSW, Sydney, NSW, Australia[d] Institut de Génétique et de Biologie Moléculaire et Cellulaire, Centre National de la Recherche Scientifique/Institut National de la Santé et de la Recherche Médicale/Université de Strasbourg, Illkirch, France[e] Department of Pharmacology, Innsbruck Medical University, Innsbruck, Austria[f] St. Vincent's Hospital Clinical School, University of New South Wales, Kensington, NSW, Australia[g] School of Medical Sciences, University of New South Wales, Kensington, NSW, Australia

Abstract

Chronic opiate usage, whether prescribed or illicit, has been associated with changes in bone mass and is a recognized risk factor for the development of osteoporosis; however, the mechanism behind this effect is unknown. Here we show that lack of dynorphin, an endogenous opioid, in mice (Dyn−/−), resulted in a significantly elevated cancellous bone volume associated with greater mineral apposition rate and increased resorption indices. A similar anabolic phenotype was evident in bone of mice lacking dynorphin's cognate receptor, the kappa opioid receptor. Lack of opioid receptor expression in primary osteoblastic cultures and no change in bone cell function after dynorphin agonist treatment *in vitro* indicates an indirect mode of action. Consistent with a hypothalamic action, central dynorphin signaling induces extracellular signal-regulated kinase (ERK) phosphorylation and c-fos activation of neurons in the arcuate nucleus of the hypothalamus (Arc). Importantly, this signaling also leads to an increase in Arc NPY mRNA expression, a change known to decrease bone formation. Further implicating NPY in the skeletal effects of dynorphin, Dyn−/−/NPY−/− double mutant mice showed comparable increases in bone formation to single mutant mice, suggesting that dynorphin acts upstream of NPY signaling to control bone formation. Thus the dynorphin system, acting via NPY, may represent a pathway by which higher processes including stress, reward/addiction and depression influence skeletal metabolism. Moreover, understanding of these unique interactions may enable modulation of the adverse effects of exogenous opioid treatment without directly affecting analgesic responses.

1. Introduction

The opioid family is complex, consisting of more than 20 peptides derived from three independent genes, proopiomelanocortin (POMC), proenkephalin (PENK), and prodynorphin (PDyn) (Boer and Van Minnen, 1985). These genes produce inactive polypeptide precursors that are activated following tissue-specific processing. In the case of the prodynorphin precursor, processing produces six dynorphins: dynorphin A, dynorphin B, alpha- and beta-neoendorphin, leumorphine and big dynorphin (Han and xie, 1982). Dynorphin is produced almost exclusively in the CNS, including the hypothalamus (Lin et al., 2006). Pharmacologically, dynorphins preferentially bind to the kappa-opioid receptor (KOR), but they also bind with reduced affinity to mu-opioid receptors (MOR) and delta-opioid receptors (DOR) (Mansour et al., 1995). While opiate analgesia is the result of activation of MOR signaling (Matthes et al., 1996), both dynorphin and KOR expression are elevated by chronic opiate exposure (Wang et al., 1999) indicating that chronic opiate use may involve responses from multiple opioid receptors, including the dynorphin/KOR system.

Opioids are critical agents for pain management but chronic use is associated with adverse side effects including an increased risk for the development of osteoporosis, affecting people of all ages, not just the elderly (Daniell et al., 2006 and Shorr et al., 1992). Several

mechanisms have been proposed to explain the increase in fracture evident following opiate exposure. In men, opiates may induce androgen deficiency, due to inhibition of gonoadotrophin release from the hypothalamus and subsequent reduction of testosterone synthesis (Daniell et al., 2006). A recent study in people with an average duration of 2.5 years opiate treatment for non-malignant pain found clinically significant hypogonadism in over 25% of men. Of these hypogonadal men, 50% had bone mass in the osteopenic or osteoporotic range (Fortin et al., 2008). However, central opioid effects on gonadal steroid production is not the only factor contributing to bone loss, as the same study found 42% of men had a testosterone level that was in the normal range but were osteopenic or osteoporotic. In women, a large cohort study of elderly individuals using opiates for pain management reported the age-adjusted risk of fracture was elevated for any non-spine (HR 1.76) and hip (HR 2.12) fracture (Ensrud et al., 2003). These associations were still evident following adjustment for potential confounders including dizziness, gait speed, cognitive function and femoral neck bone mineral density (BMD), further indicating a unique opiate effect on bone. These findings are also consistent with a case-control study (Shorr et al., 1992), which reported a 1.6-fold increase in the risk of hip fracture among current users of opioid analgesics, and a prospective cohort study which found a 2-fold risk of hip fracture in users of opioid analgesics (Guo et al., 1998). Indeed, opiate-associated osteoporosis is now sufficiently recognized that routine bone density screening is being proposed for those on chronic opiate treatment for pain (Fortin et al., 2008). Despite this growing concern, the mechanism behind opiate-induced osteoporosis remains poorly defined.

Interestingly, mouse models have shown that loss of dynorphin signaling reduces neuropeptide Y (NPY) expression in the arcuate nucleus of the hypothalamus (Arc) (Sainsbury et al., 2007 and Wittmann et al., 2009). Importantly, alterations in hypothalamic NPY, acting through the Arc, have previously been demonstrated to exert powerful effects upon bone mass and osteoblast activity. Arcuate-specific elevation of NPY expression induces marked reduction in osteoblast activity (Baldock et al., 2005) and acted to correct the increased bone mass following germline NPY ablation (Baldock et al., 2009). The relationship between opioid signaling and NPY was clearly demonstrated in feeding studies with NPY-induced feeding being dose-dependently reduced by pretreatment with kappa opioid receptor antagonist or kappa antisense probes (Israel et al., 2005), demonstrating the downstream actions of dynorphin signaling in mediating NPY effects on feeding. A similar interaction between dynorphin and NPY has been demonstrated in other brain regions, with over 50% of NPY-ergic neurons in some hippocampal regions expressing the dynorphin-specific kappa opioid receptor (Racz and halasy, 2002). In light of these findings, we hypothesized that the opiate system, acting through dynorphin, may mediate its effect on bone through a central circuit involving the NPY pathway. To investigate this we generated a series of transgenic mouse models and studied their effects on bone homeostasis in vivo and in vivo.

2. Materials and methods

2.1. Animals

Dynorphin knockout mice (Dyn−/−) and neuropeptide Y knockout mice (NPY−/−) were generated and maintained as previously published (Loacker et al., 2007 and Karl et al., 2008). The dynorphin knockout leads to deletion of the entire prodynorphin gene including the initiation start codon, thereby eliminating all six potential dynorphin peptides. Double (Dyn−/−NPY−/−) knockout mice were generated by crossing Dyn and NPY single knockout mice and subsequently crossing of the double heterozygous mice. Bone tissue from KOR−/− mice (Simonin et al., 1998) were kindly provided by Prof. Kieffer, University of Strasbourg. Littermate controls were used where possible. Mice were fed a normal chow diet *ad libitum* (6% calories from fat, 21% calories from protein, 71% calories from carbohydrate, 2.6 kcal/g; Gordon's Specialty Stock Feeds, Yanderra, New South Wales, Australia). All research and animal care procedures were approved by the Garvan Institute/St. Vincent's Hospital Animal Experimentation Ethics Committee and were in agreement with the Australian Code of Practice for the Care and Use of Animals for Scientific Purpose. Mice were housed under conditions of controlled temperature (22 °C) and illumination (12-h light, 12-h dark cycle, lights on at 0700 h).

2.2. Statistical analyses

Values are presented as mean ± standard error (SEM), and statistical comparisons were

made using a two-tailed student's *t*-test, or one-way ANOVA and Bonferroni post hoc tests when an overall significant difference was detected. *p* values <0.05 were considered statistically significant.

2.3. Analysis of body composition

Mice were anesthesised with 100 mg/kg ketamine and 20 mg/kg xylazine (Parke Davis-Pfizer, Sydney, Australia; and Bayer, Leverkusen, Germany) and then scanned for whole body bone mineral density (BMD) and bone mineral content (BMC), lean mass, fat mass and percentage of fat using dual energy X-ray absorptiometry (DXA), (Lunar PIXImus2 mouse densitometer; GE Healthcare, WI). Following cull by cervical dislocation and decapitation, isolated femoral scans were conducted on defleshed femurs.

2.4. Bone histomorphometry

Mice were injected with the fluorophor calcein (Sigma Chemical Company, St. Louis, USA) at 20 mg/kg (s.c.), 10 and 3 days prior to collection. Mice were killed by cervical dislocation between 10.00–14.00 h for tissue collection. Both femora and the lumbar spine were excised and fixed in 4% paraformaldehyde for 16 h at 4 °C. The right femur was bisected transversely at the midpoint of the long axis and the distal half embedded undecalcified in ethacrylate resin (Medim-Medizinische Diagnostik, Giessen, Germany). Sagittal sections with 5 μm thickness were analysed for osteoblastic and osteoclastic parameters, as previously described (Allison et al., 2006, Lundberg et al., 2007a and Lundberg et al., 2007b.

2.5. Micro-computed tomography

Femurs and third lumbar vertebra (L3) were assessed using micro-computed tomography (micro-CT) as described before (Baldock et al., 2009). Briefly, following fixation, left femora were cleaned of muscle and placed in a Skyscan 1174 (Skyscan, Aartselaar, Belgium). The X-ray source was set at 50 kV and 800 μA, with a 0.5 mm aluminium filter and sharpening was set to 40%. Image projections were acquired over an angular range of 180° (angular step of 0.4°) with pixel size of 6.2 μm and the exposure set to 3600 ms. The image slices were reconstructed using NRecon, which uses a modified Feldkamp algorithm (Skyscan, Aartselaar, Belgium). In vivo micro-CT scans of the third lumbar vertebra (L3) were obtained with the same manner; with the region of interest extending 20 slices from either growth plate.

2.6. Isolation and differentiation of bone marrow stromal cells

The isolation and differentiation of plastic adherent bone marrow stromal cells (BMSCs) from 5 to 9 week old mice was carried out as previously described (Lundberg et al., 2007b).

Differentiation into mineral-producing osteoblasts was achieved by culturing the cells in osteogenic media consisting of control media supplemented with 50 mg/L ascorbic acid and 10 mM ß-glycerophosphate. Alkaline phosphatase activity (ALP), a marker for early osteoblast differentiation, was visualized by ALP staining. Briefly, ALP activity in cells was detected using *p*-nitrophenylphosphate (*p*NPP) (Sigma–Aldrich, St. Louis, MO, USA) as the substrate. Mineralization of calcium deposits was assessed by von Kossa staining (2% silver nitrate staining under UV light for 30 min at room temperature), followed by multiple washes with distilled water to remove background staining (Lee et al., 2011). The extent of ALP staining or mineralisation was quantified using the Leica QWin imaging system (Leica Micro-systems, Heerbrugg, Switzerland). All samples were assayed in triplicate. Results are representative of a minimum of two independent experiments.

2.7. Isolation of calvarial osteoblastic cells

Primary calvarial osteoblasts were isolated as previously described (Jochum et al., 2000). Briefly, five calvaria from six-day-old mice were dissected, cleaned in 70% ethanol then PBS. Calvaria were then digested using 0.1% Collagenase and 0.2% Dispase II α-MEM without FCS and were shaken for 10 min at 37 °C. After incubation the upper liquid phase, (fraction 1) was discarded. This step was repeated by adding 1 ml of digestion medium, but the liquid phase (fraction 2) was recovered and collected. This step was repeated four times. The cells from fractions 2–5 were pooled by centrifugation (5 min, 500 g). The supernatant was discarded and the pellet was resuspended in 1 ml α-MEM. The cells were seeded and cultured in 6-well plates. 1.5 ml of α-MEM culture medium containing 10% FCS and antibiotics was added to each well before 1 ml of cell suspension was added and grown at 37 °C in an atmosphere of 5% CO2 in air. The medium was replaced every 3 days and the

cells were grown until sub-confluent before expanded and final use.

2.8. Isolation of neuronal cells
Pregnant female C57Bl/6 mice were imported from the Animal Resources Centre (Perth, Australia). Briefly, cerebra taken from P1-P2 pups were macerated, trypsinized (0.5% trypsin, 10 min, 37 °C/5% CO2) and triturated. The cell suspension was washed in culture media (DMEM/F12 with 10% fetal bovine serum (FBS), 1 mM sodium pyruvate, 100 U/ml penicillin, 100 mg/ml streptomycin) and cultured at 37 °C/5% CO2 in poly-d-lysine (10 mg/ml in borate buffer)-coated 75 cm^2 tissue-culture flasks. The media was changed once a week. At 10–14 days *in vitro* the mixed glial cultures were plated and used for cell signaling experiments.

2.9. RNA extraction, cDNA preparation, and RT-PCR
Marrow-intact femurs and tibias (Bo), calvaria (Ca), white adipose tissue (Ad) and whole brain (Br) were isolated from 6–10 week old mice and snap frozen. Subsequently the selected tissue was homogenized in TRIzol® reagent using a polytron. RNA extractions were carried out using TRIzol® reagent according to the manufacturer's instructions (Invitrogen).

Amplification of Dynorphin (DYN)/kappa-opioid receptor (KOR)/mu-opioid receptor (MOR) and delta-opioid receptor (DOR) PCR: initial denaturation, 94 °C, 5 min @ 35 cycles of PCR amplification: denaturation, 94 °C for 40 s, annealing 57 °C for 40 s, elongation, 72 °C for 45 s and final elongation, 72 °C, 15 min, cool off, 4 °C.
Primers: DYN-F ATGTTATGGCGGACTGCCTG, DYN-R TTTGTACAGGT CCTCATGCC; product 548 bp. KOR-F CCTGCTCTCCCAGTGCTTGC KOR-R GGTGCCTCCAAGGACTATCG; product 535 bp. DOR-F CTGTCTGCCATCCT GTCAAA, DOR-R CGATGACGGAAGATGTGGATG; product 402 bp. MOR-F CCTCTCTTCTGCCATTGGTC, MOR-R GAGGAAGTTGGGATGCAGAA; product 489 bp.

2.10. Stimulation protein extraction and Western blotting
Primary calvarial cells were serum starved over night (0.5% FBS) and treated with 100 nM kappa-opioid receptor agonist U-50,488 (Sigma–Aldrich, Sydney, NSW, Australia) for the indicated time periods.

Protein extracts were prepared as previously described (David et al., 2002). Protein concentrations were measured using Bradford (Sigma–Aldrich, Sydney, NSW, Australia). Proteins were electrophoresed on 10% SDS polyacrylamide gels and transferred to nitrocellulose membrane. The blots were probed with p44/42 MAPK (Erk1/2) antibody (Cell Signalling Technology). As a secondary antibody, anti-mouse/rabbit IgG HRP conjugate (Promega, Sydney, NSW, Australia) was used. Bands were detected by ECL (GE Healthcare Australia, Sydney, NSW, Australia).

2.11. Central agonist injection and c-fos immunohistochemistry
Wild type mice at 12 weeks of age were injected intracerebroventricularly (icv) with either 1.5 µl kappa opioid receptor agonist U-50,488 (10 µM) or control buffer at 10:00–12:00 h. Brain injection coordinates relative to Bregma were posterior 0.34 mm, lateral ±1.0 mm, ventral 2.5 mm, corresponding to the left lateral ventricle (Franklin and paxinos, 1997). To ensure the least possible variation in c-fos expression, all mice were sacrificed 60 ± 1 min after icv injection. C-fos immunohistochemistry was performed on free-floating sections as described previous (Lin et al., 2009). Comparisons were made between the two groups (three mice per group) stained at same time and the average number of neuron counts in each nucleus was determined from both left and right sides. All groups were pooled for final analysis and the differences between groups were assessed by ANOVA followed by Bonferroni post hoc tests.

2.12. Intrahypothalamic injection into mouse Arc and *in situ* hybridization
Twelve wild type mice at 15 weeks of age were divided into four groups and anesthetized with 100 and 20 mg/kg ketamine/xylazine (Parke Davis-Pfizer, Sydney, Australia and Bayer AG, Leverkusen, Germany) and placed on a Kopf stereotaxic frame (David Kopf, California, USA), with the head in the flat skull position. Mice were injected unilaterally into the arcuate hypothalamic nucleus (Arc) with 1 µl Kappa (U-50,488) (10 µM), 1 µl Mu (DAMGO) (1 mM), 1 µl Delta opioid (DPDPE) (10 mM) receptor agonists (Sigma, USA) or 1 µl PBS as control, respectively, using a 10 µl Hamilton syringe attached to Micro4 Micro Syringe Pump Controller (World Precision Instruments Inc., Sarasota, USA). Brain injection coordinates

relative to Bregma were posterior 1.94 mm, lateral ± 0.3 mm, ventral 5.6 mm, corresponding to the Arc.

All mice were culled by cervical dislocation and decapitation exactly 60 min after injection and brains were removed and immediately frozen on dry ice. Coronal sections (20 μm) were cut on a cryostat and thaw-mounted on Superfrost® slides (Menzel-Glaser, Braunschweig, Germany). Matching sections from the same coronal brain level of three opioid receptor agonists injection and PBS injection of mice (n = 3 mice/group) were assayed together using radiolabelled DNA oligonucleotides complementary to mouse *NPY* (5′-GAGGGTCAGTCCACACAGCCCCATTCGCTTGTTACCTAGCAT-3′); as described previously (Lin et al., 2006).

For evaluation of mRNA levels in scattered neurons, images from dipped sections were digitized using a ProgRes 3008 camera (Zeiss, Jena, Germany) mounted on a Zeiss Axiophot microscope (Zeiss, Jena, Germany). Silver grain density over single neurons was evaluated using NIH-Image 1.61 software (written by Wayne Rasband and available from anonymous FTP at zippy.nimh.nih.gov). Background labeling was uniform and never exceeded 5% of specific signal.

3. Results

3.1. Increased bone mass and reduced fat mass in mice lacking dynorphin expression

In order to determine a possible role for dynorphin signaling in skeletal regulation, body composition and bone content were analyzed by DXA in 16-week-old male and female wild type (WT) and Dyn−/− mice. Loss of dynorphin significantly reduced body weight, lean mass (in females only), total fat mass and percent adiposity without change in stature, as represented by femur length (Table 1). In contrast to the loss of weight, femoral bone mineral density (BMD) and bone mineral content (BMC) were greater in both sexes of Dyn−/− mice, with this change also evident in whole body BMD and whole body BMC in male mice (Table 1).

Table 1
Body composition and bone mass in Dyn−/− mice.

Characteristics	WT male (n > 15)	Dyn−/−male (n > 15)	p
Body weight (g)	30.71 ± 1.15	28.14 ± 0.51	*
Lean mass (g)	22.41 ± 0.74	22.41 ± 0.58	NS
Fat mass (g)	5.48 ± 0.52	3.25 ± 0.13	***
Adiposity (% of BW)	19.55 ± 1.40	13.14 ± 0.98	***
Isolated femur length (mm)	16.04 ± 0.14	16.11 ± 0.16	NS
Whole body BMD (mg/mm^2)	52.36 ± 0.07	57.18 ± 0.09	**
Whole body BMC (mg)	377.30 ± 1.24	431.30 ± 1.02	**
Isolated femur BMD (mg/mm^2)	61.01 ± 1.26	72.25 ± 1.84	***
Isolated femur BMC (mg)	25.33 ± 0.14	30.63 ± 0.11	*
	WTfemale(n > 15)	Dyn−/−female(n > 15)	
Body weight (g)	22.83 ± 0.61	20.15 ± 0.29	***
Lean mass (g)	17.04 ± 0.44	15.08 ± 0.22	***
Fat mass (g)	4.36 ± 0.26	2.99 ± 0.13	***
Adiposity (% of BW)	20.33 ± 1.01	16.54 ± 0.62	**
Isolated femur length (mm)	15.84 ± 0.11	15.64 ± 0.13	NS
Whole body BMD (mg/mm^2)	52.55 ± 0.06	51.00 ± 0.07	NS
Whole body BMC (mg)	339.10 ± 0.82	336.90 ± 0.83	NS
Isolated femur BMD (mg/mm^2)	53.12 ± 1.10	59.14 ± 1.51	**
Isolated femur BMC (mg)	19.80 ± 0.07	23.50 ± 0.12	*

* p < 0.05.
** p < 0.01.
*** p < 0.0001.

3.2. Loss of dynorphin signaling increases cancellous bone volume and turnover

To define the cellular changes responsible for the altered bone mass, cancellous bone of the distal femoral metaphysis was examined. In Dyn−/− mice, cancellous bone volume was

significantly increased (males 33% and females 45%), associated with increased trabecular number and trabecular thickness in both sexes (Fig. 1A–D) The greater bone volume was consistent with an increase in bone formation rate (Fig. 1E) resulting from changes in the speed of bone formation. Indeed, mineral apposition rate was an average of 45% greater than wild type, with no change in mineralising surface (Fig. 1F and G). The change in mineral apposition rate is evident in the photomicrographs (Fig. 1H). In addition, bone resorption indices were also elevated, indicating an increase in bone turnover in Dyn−/− mice. Specifically, osteoclast surface and osteoclast number were increased on average by 60% and 70%, respectively in both sexes (Fig. 1I and J). Greater bone mass in Dyn−/− mice was also evident in cortical bone, with femoral cortical area and thickness increased compared to WT (Fig. 1K–M), with a coincident increase in calculated bone strength as indicated by the significant increase in polar moment of inertia (Fig. 1N)

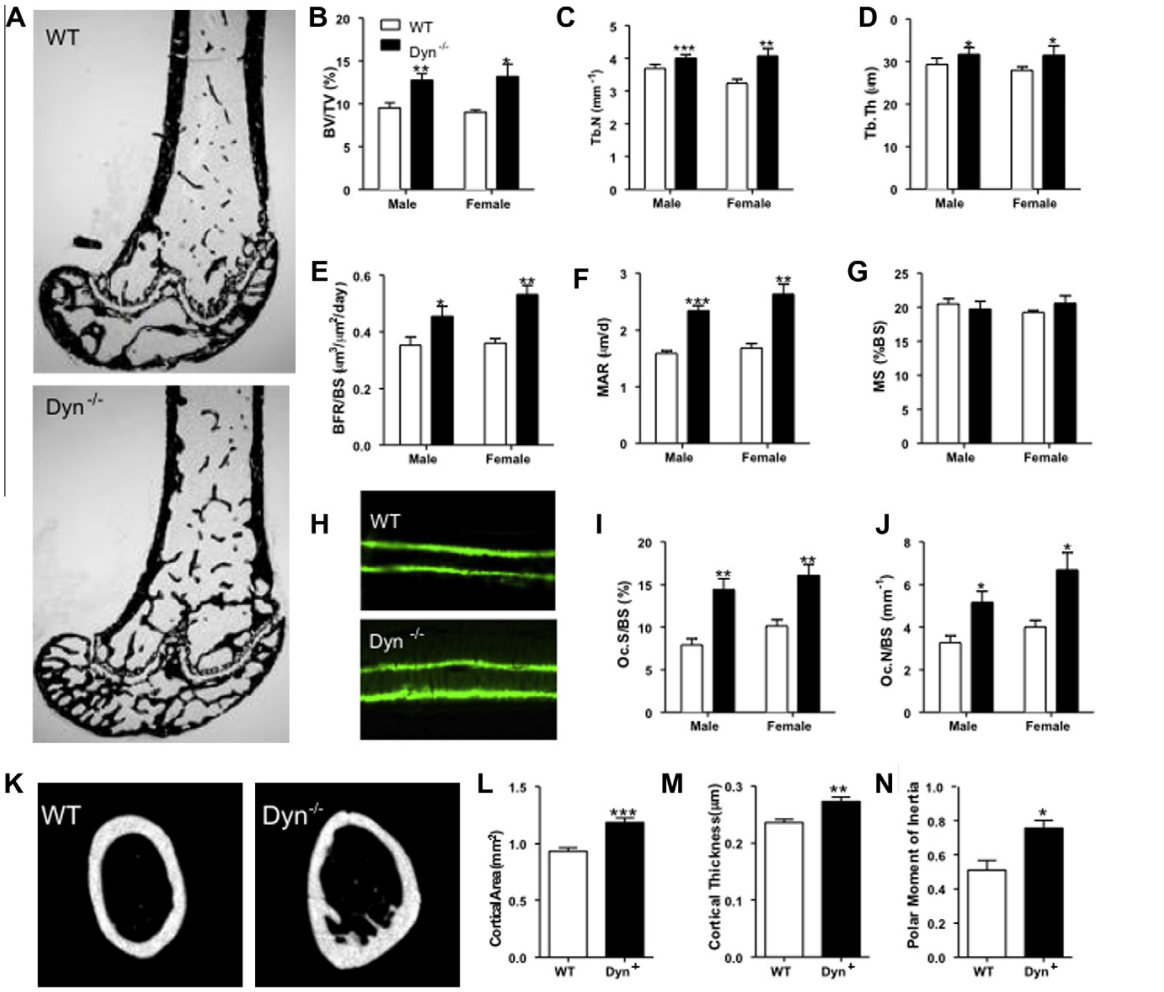

Fig. 1. Skeletal phenotype of Dyn−/− mice. (A) Photomicrographs of the distal femur of 16-week-old male wild type (WT) and dynorphin knockout (Dyn−/−) mice showing more abundant darkly stained bone in the mutant mice. (B–D) Analysis of cancellous bone in male and female WT and Dyn−/− mice revealed increased bone volume in the knockouts (B) due to greater trabecular number (C) and thickness (D). (E–G) Bone formation rate (E) was greater in Dyn−/− than in WT mice due to increased mineral apposition rate (F), with no change in mineralizing surface (G). (H) Photomicrographs showing altered mineral apposition rate in Dyn−/− versus WT mice. (I and J) Bone resorption indices were also elevated in Dyn−/− compared to WT mice, with greater osteoclast surface (I) and osteoclast number (J) in the knockouts. Data are means ± SEM of 3–15 mice per group. $^{*}p < 0.05$, $^{**}p < 0.01$, $^{***}p < 0.0001$ versus WT (K–N) Cortical bone was similarly increased in Dyn−/− mice. (K) Micro-computed tomography analysis of the mid-femoral cross-section of male mice, showed greater cortical bone area (L) and cortical thickness (M) resulting in greater calculated bending strength (N). Data are means ± SEM of 6–7 mice per group. $^{*}p < 0.05$, $^{**}p < 0.01$, $^{***}p < 0.0001$ versus WT.

3.3. Kappa opioid receptor deletion recapitulates the dynorphin null anabolic phenotype

To assess whether dynorphin regulates bone homeostasis via signaling through its preferred kappa opioid receptor (KOR), mice genetically deficient in KOR were analyzed for changes in bone homeostasis. In KOR−/− mice, cancellous bone volume was significantly increased, associated with increased trabecular number and trabecular thickness in both sexes (Fig. 2A–D,O–Q) The greater bone volume was consistent with an increase in bone formation rate (Fig. 2E) resulting from greater mineral apposition, with no change in mineralising surface

(Fig. 2F and G). The change in mineral apposition rate is evident in the photomicrographs (Fig. 2H). In contrast to Dyn−/− mice, bone resorption indices were not altered in KOR−/− (Fig. 2I and J). Consistent with the photomicrographs of KOR−/− mid femoral cross-sections (Fig. 1K), DXA analysis of femoral BMD indicated a significant increase in female mice (Fig. 1P). Both male and female KOR−/− mice exhibited a strong trend for increased femoral BMC ($p = 0.08$, $p = 0.09$, respectively) (Fig. 1Q). Thus opioid signaling through the dynorphin family of peptides, acts to tonically reduce bone formation.

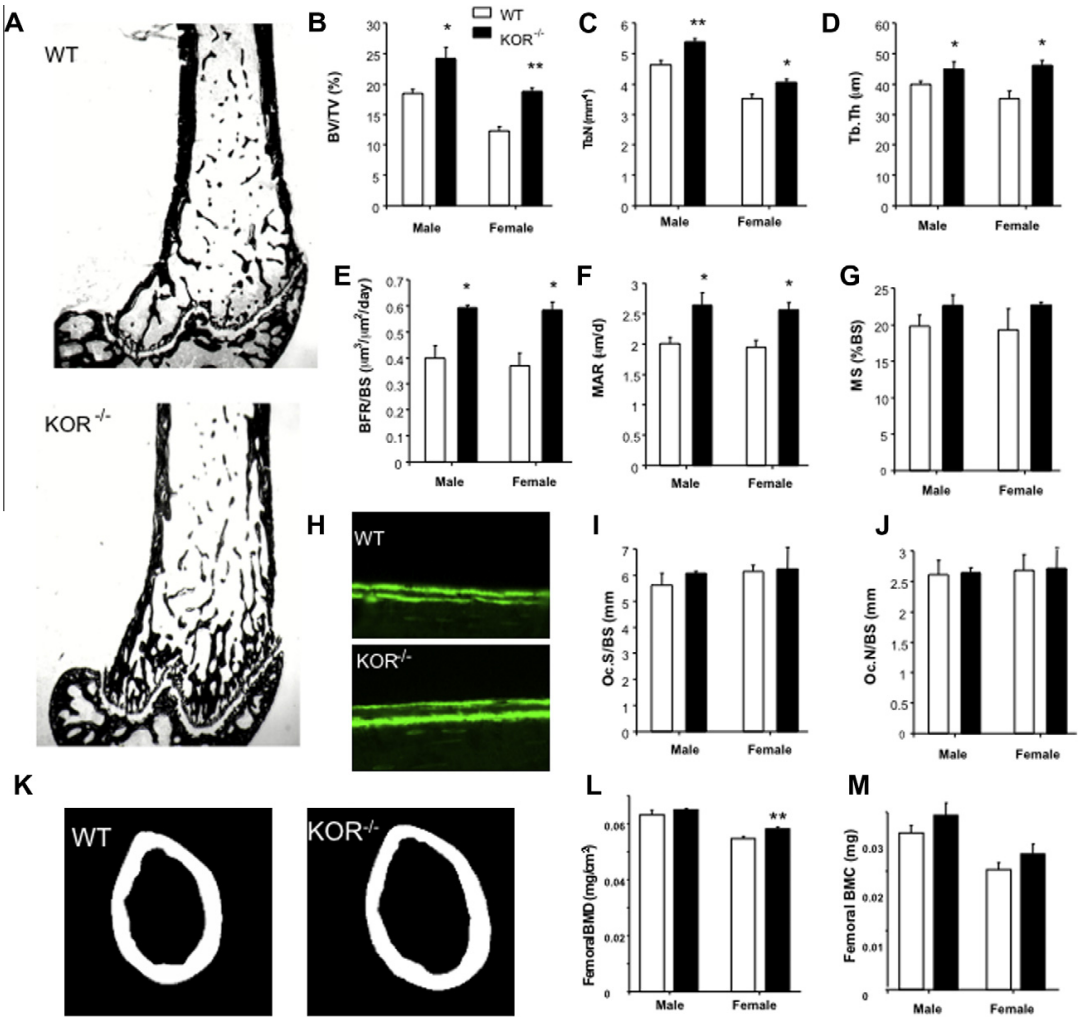

Fig. 2. Skeletal phenotype of KOR−/− mice. (Q) Kappa opioid receptor knockout mice display increased bone mass. The skeletal phenotype of KOR−/− mice recapitulates the anabolic changes in dynorphin knockout. (A) Photomicrographs of the distal femur of 16-week-old male wild type (WT) and kappa opioid receptor knockout (KOR−/−) mice showing more abundant darkly stained bone in the mutant mice. (B–D) Analysis of cancellous bone in male and female WT and KOR−/− mice revealed increased bone volume in the knockouts (B) due to greater trabecular number (C) and thickness (D). (E–G) Bone formation rate (E) was greater in KOR−/− than in WT mice due to increased mineral apposition rate (F), with no change in mineralizing surface (G). (H) Photomicrographs showing altered mineral apposition rate in KOR−/− versus WT mice. (I and J) Bone resorption indices were not elevated in KOR−/− compared to WT mice, with greater osteoclast surface (I) and osteoclast number (J) in the knockouts. (K–N) Cortical bone was similarly increased in KOR−/− mice. (K) Micro-computed tomography analysis of the mid-femoral cross-section of male mice. Femoral bone mineral density (BMD) as greater in female KOR−/− mice (L), with a consistent trend for increased (M) femoral bone mineral content (BMC) in male and female KOR−/− mice versus WT ($p = 0.08$, $p = 0.09$, respectively). Data are means ± SEM of 4 mice per group. $^{*}p < 0.05$, $^{**}p < 0.01$ versus WT.

3.4. Dynorphin does not act directly upon osteoblasts

As clearly demonstrated above, dynorphin signaling is required for normal bone homeostasis; however, the mechanism by which this opioid family alters bone cell activity is unclear. In order to define the signaling pathway by which dynorphins alter bone cell activity, we first investigated the presence of dynorphin and opioid receptor expression in bone tissue. As shown in Fig. 2A, skeletal tissues: whole bone (marrow included) (Bo) and calvarial tissue (Ca), as well as adipose tissue, exhibit no dynorphin or kappa opioid receptor expression. Indeed no expression of any of the three opioid receptors was evident in bone, with low levels of delta receptor evident in fat tissue (Fig. 3A). In contrast, dynorphin and all the opioid

receptors were strongly expressed in brain tissue. Interestingly, loss of dynorphin expression results in slightly increased expression levels of mu-opioid receptors in the brain and adipose tissue (Fig. 3A), but importantly does not alter expression patterns in skeletal tissue. Moreover, dynorphin and KOR expression are also absent from BMSC cultures from WT and Dyn−/− mice, and were not induced by FCS or NPY in serum-starved wild type cultures (Fig. 3B).

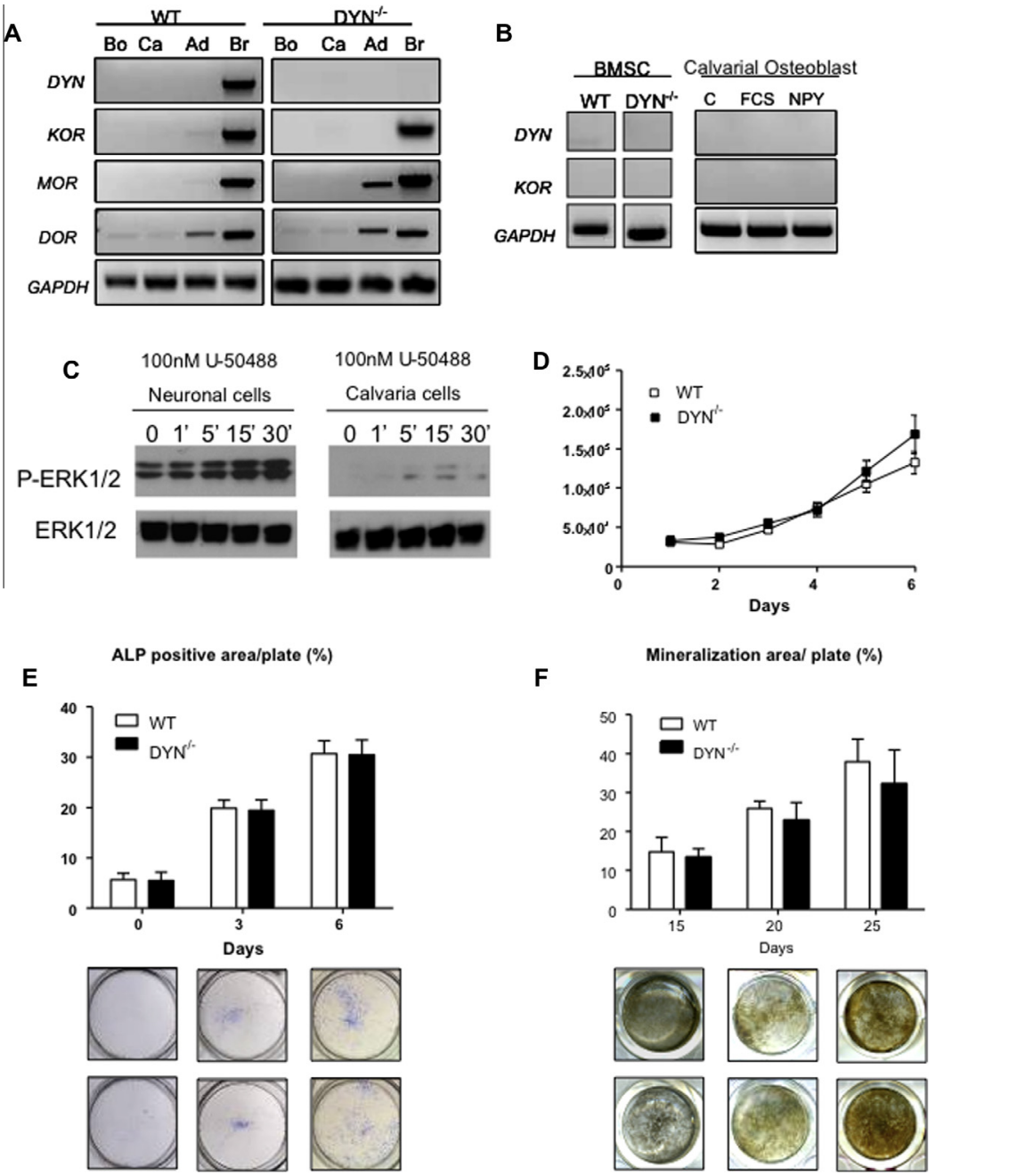

Fig. 3. No direct effects of dynorphin on bone cells. (A) Expression for dynorphin (DYN) and all three opioid receptors (kappa, KOR; mu, MOR; and delta, DOR) was present in samples of brain tissue (Br) from WT mice, but was absent from whole bone (Bo) and calvarial tissue (Ca) from WTs. WT white adipose tissue (Ad) showed expression for DOR only. Tissues from Dyn−/− mice recapitulated these WT expression patterns, with MOR as well as DOR evident in white adipose tissue, and a lack of DYN in brain. (B) DYN and KOR were absent from bone marrow stromal cell cultures (BMSC) and could not be induced in starved cells by addition of fetal calf serum (FCS) or neuropeptide Y (NPY) in primary calvarial osteoblasts. (C) The kappa agonist U-50,488 induced signaling in neuronal cells via rapid phosphorylation of ERK, but not in calvarial osteoblasts. (D) Proliferation of primary osteoblastic cultures was not different between WT and Dyn−/− cells. (E and F) Differentiation is not altered in Dyn−/− cells, as indicated by the observation that alkaline phosphatase (E) and mineralization (F) were similar in primary osteoblast cultures from WT and Dyn−/− mice.

To further exclude the possibility of a direct action of dynorphin and KOR receptor signaling, we treated mouse primary osteoblasts and primary neuronal cells with U-50,488, a KOR-specific agonist (Simonin et al., 1998), and compared P-ERK activation. Consistent with

kappa opioid receptor expression, sustained activation of P-ERK is evident in neuronal cells, however activation of ERK phosphorylation was virtually absent in osteoblastic cells (Fig. 3C). In addition, we also investigated the effect of dynorphin deficiency on osteogenic proliferation and differentiation by assessing the ability of primary calvarial osteoblastic cultures isolated from Dyn−/− mice to differentiate into mature, mineral-producing osteoblasts *in vitro*. There was no difference in proliferation efficiency between the Dyn−/− and control cultures (Fig. 3D). Differentiation, following plating in osteogenic media, was assessed by alkaline phosphatase production and mineralization, which were not different between WT and Dyn−/− cultures as evident by the photomicrographs (Fig. 3E and F). Taken together, these results strongly suggest that dynorphin's effect on bone does not involve a direct action on osteoblast, but rather involve an indirect pathway.

3.5. Dynorphin regulates NPY expression via kappa opioid action

As direct action of dynorphin on bone tissue does not seem to explain the altered bone phenotype in Dyn−/− mice, we focused our attention on potential indirect mechanisms via the central nervous system. To test this we injected kappa opioid agonist U-50,488 icv into mouse brains and evaluated the activation of neurons indicated by c-fos activity (Fig. 4A). KOR agonist injection induced a strong and specific activation of neurons in the Arc of the hypothalamus, with 37 ± 6 positive staining neurons in the Arc of agonist-injected mice compared to 10 ± 2 in the Arc of control-injected mice; (n = 3, p = 0.003).

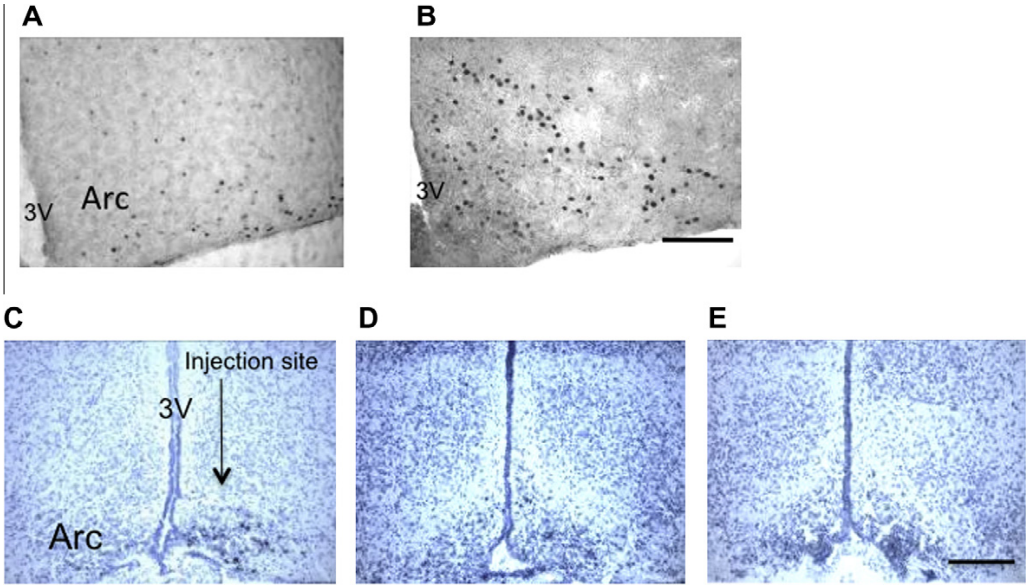

Fig. 4. KOR agonist-specific changes in the hypothalamus. (A and B) ICV injection of the KOR specific agonist U-50,488 strongly increases c-fos activation of arcuate hypothalamic (Arc) neurons (B) compared to control saline-injected mice (A). Bar represents 120 μm. (C) Unilateral Arc injection of the KOR-specific agonist U-50,488 results in strong upregulation of NPY mRNA on the injected side but not on the contralateral control side. (D) Injection of either the MOR-specific agonist DAMGO or (E) the DOR-specific agonist DPDPE have no effect on NPY mRNA expression in the Arc. n = 3, bar represents 60 μm.

We have shown previously that lack of dynorphin signaling leads to reduced expression of neuropeptide Y in the Arc (Sainsbury et al., 2007 and Wittmann et al., 2009), which would be expected to result in a NPY-induced increase in bone mass and provide a mechanism for dynorphins action on bone (Baldock et al., 2005, Baldock et al., 2009, Baldock et al., 2002 and Baldock et al., 2006). In order to test this hypothesis we injected KOR (U-50,488), DOR (DPDPE) and MOR (DAMGO) receptor-specific agonists unilaterally into the arcuate nucleus of wild type mice and measured changes in NPY mRNA expression by *in situ* hybridization between injected and contralateral sides of the Arc. Interestingly, silver grain density over single neurons on the injected side of the Arc was significantly increased 2.8-fold in mice injected with the Kappa opioid receptor agonist (1143 ± 201) compared to the intra-hypothalamic contra lateral Arc control side (402 ± 49), (n = 3; p < 0.005); (Fig. 3C). Importantly, no significant changes were found in the Arc of mu and delta opioid receptor agonist (Fig. 4D and E) or saline injected control groups. This clearly indicates that dynorphin signaling through its preferred kappa receptor increases NPY expression, which has been

shown to result in decreased bone formation (Baldock et al., 2002, Baldock et al., 2005 and Baldock et al., 2006)

3.6. Bone homeostasis following coincident loss of dynorphin and neuropeptide Y signaling
The involvement of NPY-mediated processes in the skeletal phenotype of Dyn−/− mice was further explored by comparison of Dyn−/− with NPY−/− mice and Dyn−/−NPY−/− double delete mice. In the distal femoral metaphysis cancellous bone volume was similarly elevated in Dyn−/− and NPY−/− mice (Fig. 5A). Importantly, Dyn−/−NPY−/− mice displayed equivalently increased cancellous bone volume, with no difference between the three mutant genotypes (Fig. 5B). Moreover, trabecular number was similarly increased in the mutant mice, consistent with equivalent increases in mineral apposition rate (Fig. 5E). The increase in mineralizing surface was not significant in NPY−/− mice, as a result bone formation rate was only significantly elevated in Dyn−/− and Dyn−/−NPY−/− models (Fig. 5F and G). Bone resorption indices were also similarly altered, with greater osteoclast number and surface in the three mutant groups compared to wild type mice (Fig. 5H and I). In contrast, in lumbar vertebra, NPY−/− mice were the only group to show a significant skeletal change. Critically, the similarity in bone homeostasis between dynorphin and NPY deficiency provide further evidence for a single pathway to bone.

4. Discussion

Discovery of the scope and strength of neural influences upon skeletal tissue has been an important advance in bone biology in recent years (Driessler and Baldock, 2010). Further expanding these unique neuro/skeletal relationships, here we identify a novel interaction between the opioid system and bone demonstrating an inhibitory action of dynorphins on skeletal tissue, acting through kappa opioid receptors. In particular, loss of dynorphins, one of the three endorphin ligand families, induces a skeleton-wide increase in bone mass thereby revealing for the first time a connection between opioid signaling and bone mass regulation. Moreover, this increase in bone mass in dynorphin knockout animals is most likely due to a lack of kappa-mediated stimulation of hypothalamic neuropeptide Y expression. In this manner, upregulation of dynorphin and kappa receptor expression, known to occur in response to chronic opiate exposure (Wang et al., 1999), may increase central NPY expression and – given the known role of hypothalamic NPY expression to inhibit bone (Baldock et al., 2009, Baldock et al., 2002, Baldock et al., 2006 and Allison et al., 2006) – thereby suppress bone formation and reduce bone mass and strength. Importantly, inhibition of this pathway may enable attenuation of the skeletal side-effects of chronic opiate exposure, without modulation of the analgesic effects, which occur predominantly through the mu-opioid receptor.

Dynorphin signaling has been implicated in numerous processes including stress and depression, as well as epilepsy and energy homeostasis (Sainsbury et al., 2007 and Schwarzer, 2009). The current study is the first to identify dynorphin actions in the regulation of bone mass and provides a potential link to known opioid side-effects on bone. Complete inhibition of dynorphin production was associated with an increase in bone mass, in both male and female mice, with a significant increase in calculated bone strength. This change was coincident with increased activity of both bone-forming osteoblastic and bone-resorbing osteoclastic bone cell lineages. Both bone formation and bone resorption were increased, with osteoclasts being more common on bone surfaces in Dyn−/− mice. Critically, bone formation was increased to a greater degree than bone resorption, with increases in the rate at which the bone mineral apposition process occurred, and resulting in a net gain in bone mass.

Opioid signaling is complex, with numerous ligands acting across several opioid receptors, and abundant expression in central and peripheral nervous tissue. However, expression of dynorphin and its cognate receptor, the kappa opioid receptor, were not detected in primary osteoblastic cultures or whole bone extracts. This result strongly suggested a non-local action of dynorphin on bone. Several additional lines of evidence were consistent with this hypothesis. Firstly, all opioid receptors and dynorphin were expressed in brain extracts, and dynorphin agonist treatment induced robust signaling in neuronal cells;

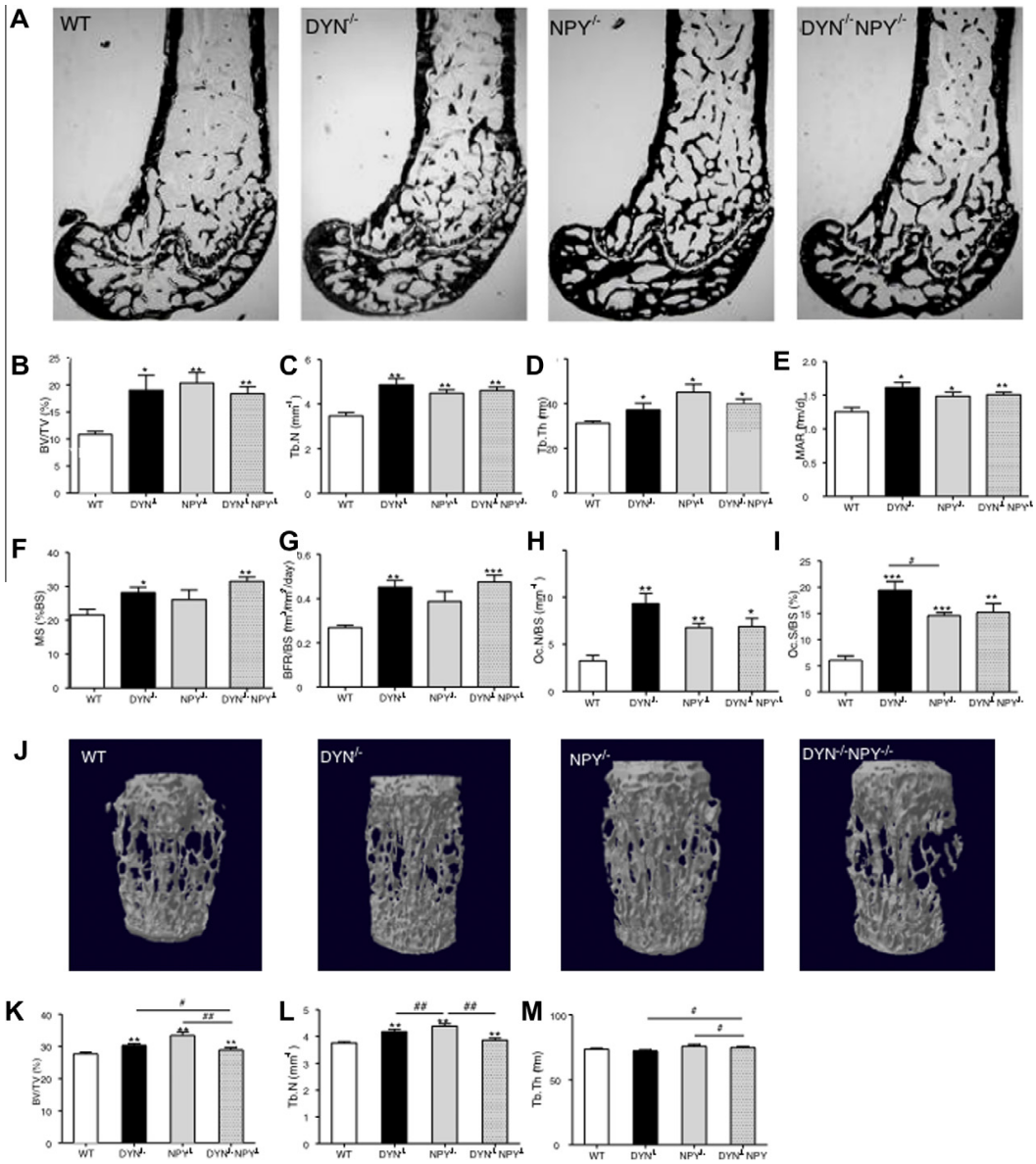

Fig. 5. Similar skeletal effects of dynorphin and neuropeptide Y deletion. (A) Photomicrographs showing that loss of Dyn or NPY increased bone mass in male mice, but dual mutants do not display greater bone mass then single mutants. (B) Cancellous bone volume and trabecular number (C) were similarly elevated in the three mutant genotypes, with an increase in trabecular thickness (D) only in NPY−/− and Dyn−/−NPY−/− double mutants. Mineral apposition rate (E) was equally elevated in the three knockout models, but mineralizing surface (F) and bone formation rate (G) were only significantly elevated in Dyn−/− and DYN−/−NPY−/− mice. Bone resorption indices osteoclast surface (H) and osteoclast number (I) were also elevated in all mutant genotypes. (J–M) In lumbar vertebrae, as evident in the micro-computed tomography images (J), loss of NPY but not Dyn increased cancellous bone volume (K) and trabecular number (L) with no change in trabecular thickness (M). Data are means ± 7–10 mice per group. $^{*}p < 0.05$, $^{**}p < 0.01$, $^{***}p < 0.0001$ versus WT, $^{\#}p < 0.05$, $^{\#\#}p < 0.01$ for the comparison indicated by horizontal bars.

however this was not the case in primary osteoblastic cells. Moreover, primary osteoblastic cultures from Dyn−/− mice did not differ from those from wild type with respect to proliferation potential, or the ability of differentiated cells to produce alkaline phosphatase in early culture or to produce mineralized nodules in late stage cultures. Thus, the dynorphin effect on the skeleton does not appear to result from a direct action on the cells of bone or to involve a constitutive change in osteoblast activity.

In the absence of direct dynorphin signaling, a central axis to bone seems likely. Consistent with this, a generalised exposure of central tissues to a KOR agonist induced neural activity in the Arc, a region of the hypothalamus that is known to regulate bone mass (Baldock et al., 2002 and Elefteriou et al., 2003). Moreover, intra-nuclear injection of kappa agonist specifically into the Arc increased the expression of NPY in this hypothalamic nucleus. However, this response was absent for mu or delta agonism, indicating a dynorphin/kappa specific activation of NPY in the Arc. Importantly, NPY-ergic neurons in the hypothalamus have been demonstrated to directly alter bone mass, with an Arc-specific

increase in NPY expression producing a powerful inhibition of osteoblast activity and reduction in bone mass (Baldock et al., 2005 and Baldock et al., 2009). Furthermore, a reduction in NPY signaling, as evident in Dyn−/− mice (Baldock et al., 2005, Baldock et al., 2009, Baldock et al., 2002 and Baldock et al., 2006), is associated with greater bone mass and osteoblast activity and calculated bone strength. These data suggest that the increase in bone mass in Dyn−/− mice is likely to be a consequence of the reduction in central NPY expression, and may thus represent an indirect pathway for dynorphin control of bone mass, similar to that reported for dynorphin control of anxiety via NPY-ergic signaling (Wittmann et al., 2009). Moreover, this data also implicates increased NPY expression, likely induced by greater kappa opioid receptor signaling may represent a possible factor inhibiting bone strength under conditions of chronic opiate use. The role for altered hypothalamic NPY expression in the regulation of bone mass by opioid signaling is further supported by the similarity of skeletal effects in NPY−/−Dyn−/− mice compared to single NPY−/− and Dyn−/− knockout mice, suggesting that dynorphin/kappa signaling may act upstream of NPY. This similarity was not evident in the vertebrae, suggesting differential homeostasis between axial and appendicular skeletons, as demonstrated in other hypothalamic models (Hamrick et al., 2004).

Opioid usage is associated with marked skeletal side effects, with fracture rates significantly elevated following treatment (Ensrud et al., 2003). The mechanism involved in this reduced bone strength is poorly defined, but processes within the hypothalamus have been implicated (Daniell, 2002). Clinically relevant opioid analgesics exert their analgesic actions predominantly through MOR (Matthes et al., 1996). However, opiate exposure increases both dynorphin expression and that of its cognate receptor, KOR. Thus, in addition to MOR signaling, KOR pathways are also stimulated by these drugs, and have been shown to mediate, depressive and dysphoric states in these individuals (Pfeiffer et al., 1986 and Carlezon et al., 1998) and in Dyn−/− mice (Wittmann et al., 2009). As outlined herein, such an opiate-mediated increase in dynorphin signaling would also act to stimulate NPY expression within the hypothalamus and with it suppression of bone formation. Such alterations in hypothalamic neuropeptide activity have been noted previously, with morphine treatment reducing pro-opiomelanocortin (POMC) expression in the hypothalamus of rats (Zhou et al., 1999). Thus, in addition to well recognized endocrine actions (Fortin et al., 2008) opiate exposure may, through stimulation of dynorphin/KOR indirectly suppress osteoblast activity through activation of central neuropeptide signaling and subsequent efferent neural pathways, as proposed in Fig. 6.

While the current study defines NPY as an indirect pathway altering bone mass in situations of altered opioid signaling, endocrine pathways have also been suggested. The hypogonadism implicit in a subset of cases of opioid-induced osteoporosis has been associated with reduced gonoadotrophin release (Daniell, 2002). Dyn−/− mice however, do not show altered serum testosterone levels (Sainsbury et al., 2007) suggesting that the Dyn-mediated effects on bone are mediated independently. Moreover, a number of aspects of the Dyn−/− phenotype reinforce the lack of hypogonadism; with reduced rather than increased adiposity, no change in longitudinal bone growth, and normal breeding and litter gender balance. The reduced adiposity would reduce leptin concentrations, a known bone regulatory agent. However, several features of Dyn−/− mice are inconsistent with leptin actions. In the brain leptin deficiency results in a marked increase in NPY expression (Sainsbury et al., 2002), rather than the decrease evident in Dyn−/−; while in bone, *ob*/*ob* mice display greater cancellous but reduced cortical bone mass and long bone length (Baldock et al., 2006 and Hamrick et al., 2004) rather than the consistent increase of Dyn−/−. In the absence of an endocrine pathway, this study has therefore furthered the understanding of the mechanisms by which hypothalamic processes are involved in the skeletal response to opioid signaling and has highlighted the importance and complexity of efferent hypothalamic pathways in the peripheral responses to opioid signaling.

Taken together, this study identifies the endogenous opioid system as required for normal bone homeostasis. The dynorphin/kappa system, possibly acting via NPY, may represent a pathway by which higher processes including stress, reward/addiction and depression influence skeletal metabolism. Moreover, this may represent one axis whereby chronic opioid exposure may inhibit bone formation and strength. Modulation of these pathways could provide a novel avenue for attenuation of the adverse skeletal effects of exogenous opioid treatment, without compromising their analgesic actions.

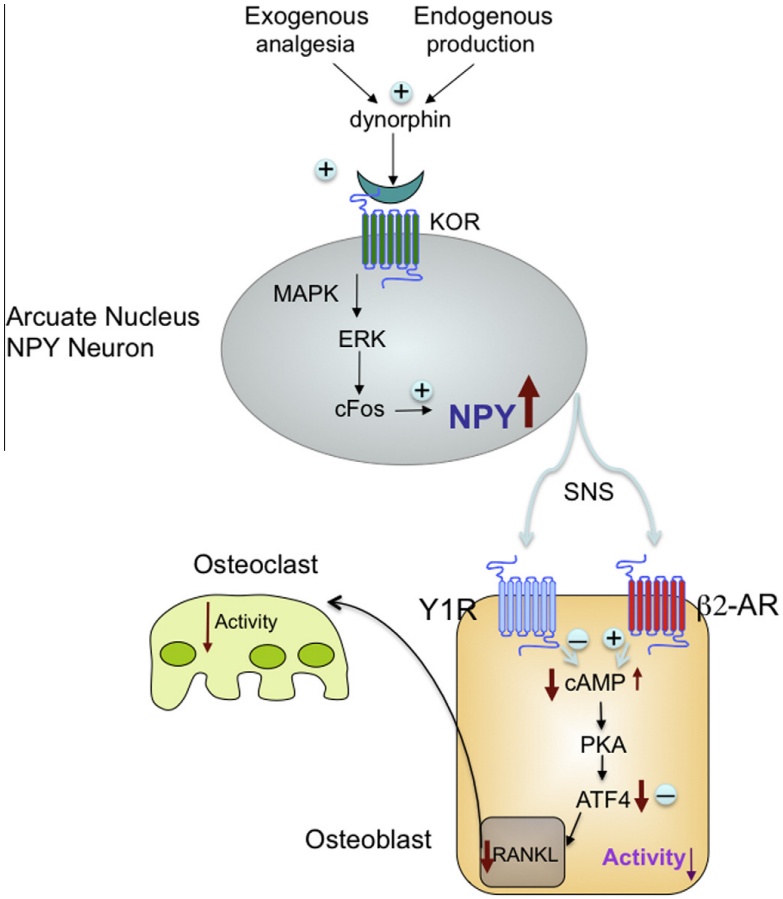

Fig. 6. Proposed mechanism for opioid-mediated suppression of bone formation. Hypothalamic Kappa opioid receptor (KOR) signaling is stimulated by endogenous dynorphin production, or exogenous opiate exposure. In turn KOR signaling leads to elevation of downstream neuropeptide Y (NPY) expression in the arcuate nucleus. Subsequent, the elevated NPY expression then acts via altering sympathetic nervous system outflow (both NPY and noradrenergic signals) to inhibit osteoblast functions and reducing bone mass.

Financial disclosure

This work has been supported by fellowships to P.B., A.S. and H.H. from the National Health and Medical Research Council (NHMRC) of Australia. The funders had no role in study design, data collection and analysis, decision to publish, or preparation of the manuscript.

Acknowledgements

We thank Audrey Matifas for excellent assistance in the kappa KO experiments. We thank the staff of the Garvan Institute Biological Testing Facility. P.B., A.S. and H.H. are supported by NHMRC of Australia, Career and Senior Research Fellowships.

References

Allison, S.J., Baldock, P., Sainsbury, A., Enriquez, R., Lee, N.J., Lin, E.J., Klugmann, M., During, M., Eisman, J.A., Li, M., Pan, L.C., Herzog, H., Gardiner, E.M., 2006. Conditional deletion of hypothalamic Y2 receptors reverts gonadectomy- induced bone loss in adult mice. J. Biol. Chem. 281, 23436–23444.

Baldock, P.A., Sainsbury, A., Couzens, M., Enriquez, R.F., Thomas, G.P., Gardiner, E.M., Herzog, H., 2002. Hypothalamic Y2 receptors regulate bone formation. J. Clin. Invest. 109, 915–921.

Baldock, P.A., Sainsbury, A., Allison, S., Lin, E.J., Couzens, M., Boey, D., Enriquez, R., During, M., Herzog, H., Gardiner, E.M., 2005. Hypothalamic control of bone formation: distinct actions of leptin and y2 receptor pathways. J. Bone Miner. Res. 20, 1851–1857.

Baldock, P.A., Allison, S., McDonald, M.M., Sainsbury, A., Enriquez, R.F., Little, D.G., Eisman, J.A., Gardiner, E.M., Herzog, H., 2006. Hypothalamic regulation of cortical bone mass: opposing activity of Y2 receptor and leptin pathways. J. Bone Miner. Res. 21, 1600–1607.

Baldock, P.A., Lee, N.J., Driessler, F., Lin, S., Allison, S., Stehrer, B., Lin, E.J., Zhang, L., Enriquez, R.F., Wong, I.P., McDonald, M.M., During, M., Pierroz, D.D., Slack, K., Shi, Y.C., Yulyaningsih, E., Aljanova, A., Little, D.G., Ferrari, S.L., Sainsbury, A., Eisman, J.A., Herzog, H., 2009. Neuropeptide Y knockout mice reveal a central role of NPY in the coordination

of bone mass to body weight. PloS One 4, e8415.

Boer, H.H., Van Minnen, J., 1985. Immunocytochemistry of peptidergic systems in the pond snail Lymnaea stagnalis. Peptides 6 (Suppl. 3), 459–463.

Carlezon Jr., W.A., Thome, J., Olson, V.G., Lane-Ladd, S.B., Brodkin, E.S., Hiroi, N., Duman, R.S., Neve, R.L., Nestler, E.J., 1998. Regulation of cocaine reward by CREB. Science 282, 2272–2275.

Daniell, H.W., 2002. Hypogonadism in men consuming sustained-action oral opioids. J. Pain 3, 377–384.

Daniell, H.W., Lentz, R., Mazer, N.A., 2006. Open-label pilot study of testosterone patch therapy in men with opioid-induced androgen deficiency. J. Pain 7, 200– 210.

David, J.P., Sabapathy, K., Hoffmann, O., Idarraga, M.H., Wagner, E.F., 2002. JNK1 modulates osteoclastogenesis through both c-Jun phosphorylation-dependent and -independent mechanisms. J. Cell Sci. 115, 4317–4325.

Driessler, F., Baldock, P.A., 2010. Hypothalamic regulation of bone. J. Mol. Endocrinol. 45, 175–181.

Elefteriou, F., Takeda, S., Liu, X., Armstrong, D., Karsenty, G., 2003. Monosodium glutamate-sensitive hypothalamic neurons contribute to the control of bone mass. Endocrinology 144, 3842–3847.

Ensrud, K.E., Blackwell, T., Mangione, C.M., Bowman, P.J., Bauer, D.C., Schwartz, A., Hanlon, J.T., Nevitt, M.C., Whooley, M.A., 2003. Central nervous system active medications and risk for fractures in older women. Arch. Intern. Med. 163, 949– 957.

Fortin, J.D., Bailey, G.M., Vilensky, J.A., 2008. Does opioid use for pain management warrant routine bone mass density screening in men? Pain Phys. 11, 539–541. Franklin, K.B.J., Paxinos, G., 1997. The Mouse Brain in Stereotaxic Coordinates. Academic Press, San Diego, pp. 35–55.

Guo, Z., Wills, P., Viitanen, M., Fastbom, J., Winblad, B., 1998. Cognitive impairment, drug use, and the risk of hip fracture in persons over 75years old: a community-based prospective study. Am. J. Epidemiol. 148, 887–892.

Hamrick, M.W., Pennington, C., Newton, D., Xie, D., Isales, C., 2004. Leptin deficiency produces contrasting phenotypes in bones of the limb and spine. Bone 34, 376– 383.

Han, J.S., Xie, C.W., 1982. Dynorphin: potent analgesic effect in spinal cord of the rat. Life Sci. 31, 1781–1784.

Israel, Y., Kandov, Y., Khaimova, E., Kest, A., Lewis, S.R., Pasternak, G.W., Pan, Y.X., Rossi, G.C., Bodnar, R.J., 2005. NPY-induced feeding: pharmacological characterization using selective opioid antagonists and antisense probes in rats. Peptides 26, 1167–1175.

Jochum, W., David, J.P., Elliott, C., Wutz, A., Plenk Jr., H., Matsuo, K., Wagner, E.F., 2000. Increased bone formation and osteosclerosis in mice overexpressing the transcription factor Fra-1. Nat. Med. 6, 980–984.

Karl, T., Duffy, L., Herzog, H., 2008. Behavioural profile of a new mouse model for NPY deficiency. Eur. J. Neurosci. 28, 173–180.

Lee, N.J., Nguyen, A.D., Enriquez, R.F., Doyle, K.L., Sainsbury, A., Baldock, P.A., Herzog, H., 2011. Osteoblast specific Y1 receptor deletion enhances bone mass. Bone 48, 461–467.

Lin, S., Boey, D., Lee, N., Schwarzer, C., Sainsbury, A., Herzog, H., 2006. Distribution of prodynorphin mRNA and its interaction with the NPY system in the mouse brain. Neuropeptides 40, 115–123.

Lin, S., Shi, Y.C., Yulyaningsih, E., Aljanova, A., Zhang, L., Macia, L., Nguyen, A.D., Lin, E.J., During, M.J., Herzog, H., Sainsbury, A., 2009. Critical role of arcuate Y4 receptors and the melanocortin system in pancreatic polypeptide-induced reduction in food intake in mice. PloS One 4, e8488.

Loacker, S., Sayyah, M., Wittmann, W., Herzog, H., Schwarzer, C., 2007. Endogenous dynorphin in epileptogenesis and epilepsy: anticonvulsant net effect via kappa opioid receptors. Brain 130, 1017–1028.

Lundberg, P., Koskinen, C., Baldock, P.A., Lothgren, H., Stenberg, A., Lerner, U.H., Oldenborg, P.A., 2007a. Osteoclast formation is strongly reduced both in vivo and in vitro in the absence of CD47/SIRPalpha-interaction. Biochem. Biophys. Res. Commun. 352, 444–448.

Lundberg, P., Allison, S.J., Lee, N.J., Baldock, P.A., Brouard, N., Rost, S., Enriquez, R.F., Sainsbury, A., Lamghari, M., Simmons, P., Eisman, J.A., Gardiner, E.M., Herzog, H., 2007b. Greater bone formation of Y2 knockout mice is associated with increased osteoprogenitor numbers and altered Y1 receptor expression. J. Biol. Chem. 282, 19082–19091.

Mansour, A., Hoversten, M.T., Taylor, L.P., Watson, S.J., Akil, H., 1995. The cloned mu, delta and kappa receptors and their

endogenous ligands: evidence for two opioid peptide recognition cores. Brain Res. 700, 89–98.

Matthes, H.W., Maldonado, R., Simonin, F., Valverde, O., Slowe, S., Kitchen, I., Befort, K., Dierich, A., Le Meur, M., Dolle, P., Tzavara, E., Hanoune, J., Roques, B.P., Kieffer, B.L., 1996. Loss of morphine-induced analgesia, reward effect and withdrawal symptoms in mice lacking the mu-opioid-receptor gene. Nature 383, 819–823.

Pfeiffer, A., Brantl, V., Herz, A., Emrich, H.M., 1986. Psychotomimesis mediated by kappa opiate receptors. Science 233, 774–776.

Racz, B., Halasy, K., 2002. Kappa opioid receptor is expressed by somatostatin- and neuropeptide Y-containing interneurons in the rat hippocampus. Brain Res. 931, 50–55.

Sainsbury, A., Schwarzer, C., Couzens, M., Herzog, H., 2002. Y2 receptor deletion attenuates the type 2 diabetic syndrome of ob/ob mice. Diabetes 51, 3420– 3427.

Sainsbury, A., Lin, S., McNamara, K., Slack, K., Enriquez, R., Lee, N.J., Boey, D., Smythe, G.A., Schwarzer, C., Baldock, P., Karl, T., Lin, E.J., Couzens, M., Herzog, H., 2007. Dynorphin knockout reduces fat mass and increases weight loss during fasting in mice. Mol. Endocrinol. 21, 1722–1735.

Schwarzer, C., 2009. 30 years of dynorphins – new insights on their functions in neuropsychiatric diseases. Pharmacol. Ther. 123, 353–370.

Shorr, R.I., Griffin, M.R., Daugherty, J.R., Ray, W.A., 1992. Opioid analgesics and the risk of hip fracture in the elderly: codeine and propoxyphene. J. Gerontol. 47, M111–M115.

Simonin, F., Valverde, O., Smadja, C., Slowe, S., Kitchen, I., Dierich, A., Le Meur, M., Roques, B.P., Maldonado, R., Kieffer, B.L., 1998. Disruption of the kappa-opioid receptor gene in mice enhances sensitivity to chemical visceral pain, impairs pharmacological actions of the selective kappa-agonist U-50,488H and attenuates morphine withdrawal. EMBO J. 17, 886–897.

Wang, X.M., Zhou, Y., Spangler, R., Ho, A., Han, J.S., Kreek, M.J., 1999. Acute intermittent morphine increases preprodynorphin and kappa opioid receptor mRNA levels in the rat brain. Brain Res. Mol. Brain Res. 66, 184–187.

Wittmann, W., Schunk, E., Rosskothen, I., Gaburro, S., Singewald, N., Herzog, H., Schwarzer, C., 2009. Prodynorphin-derived peptides are critical modulators of anxiety and regulate neurochemistry and corticosterone. Neuropsychopharmacology 34, 775–785.

Zhou, Y., Spangler, R., Maggos, C.E., Wang, X.M., Han, J.S., Ho, A., Kreek, M.J., 1999. Hypothalamic-pituitary-adrenal activity and pro-opiomelanocortin mRNA levels in the hypothalamus and pituitary of the rat are differentially modulated by acute intermittent morphine with or without water restriction stress. J. Endocrinol. 163, 261–267.